Pergamon

Geochimica et Cosmochimica Acta, Vol. 68, No. 18, pp. 3657–3664, 2004

0016-7037/04 $30.00 + .00

doi:10.1016/j.gca.2004.03.018

A Donnan potential model for metal sorption onto *Bacillus subtilis*

NATHAN YEE,[1,2,*] DAVID A. FOWLE,[3] and F. GRANT FERRIS[2]

[1]School of Earth Sciences, University of Leeds, Leeds LS2 9JT, United Kingdom
[2]Department of Geology, University of Toronto, Toronto, Canada, M5S 3B1
[3]Department of Earth Sciences, University of Windsor, Windsor, Canada, N9B 3P4

(*Received September* 22, 2003; *accepted in revised form March* 18, 2004)

Abstract—In this study, we conducted electrophoretic mobility, potentiometric titration, and metal sorption experiments to investigate the surface charge characteristics of *Bacillus subtilis* and the electrostatic interactions between metal cations and the cell surface electric field. Electrophoretic mobility experiments performed as a function of pH and ionic strength show an isoelectric point of pH 2.4, with the magnitude of the electrokinetic potential increasing with increasing pH, and decreasing with increasing ionic strength. Potentiometric titration experiments conducted from pH 2.4 to 9 yield an average surface charge excess of 1.6 μmol/mg (dry mass). Corresponding cell wall charge density values were used to calculate the Donnan potential (Ψ_{DON}) as function of pH and ionic strength. Metal sorption experiments conducted with Ca(II), Sr(II), and Ba(II) exhibit strong ionic strength dependence, suggesting that the metal ions are bound to the bacterial cell wall via an outer-sphere complexation mechanism. Intrinsic metal sorption constants for the sorption reactions were determined by correcting the apparent sorption constant with the Boltzmann factor. A 1:2 metal–ligand stoichiometry provides the best fit to the experimental data with log K_2^{int} values of 5.9 $\pm$ 0.3, 6.0 $\pm$ 0.2, 6.2 $\pm$ 0.2 for Ca(II), Sr(II), and Ba(II) respectively. Electrophoretic mobility measurements of cells sorbed with Ca(II), Sr(II), and Ba(II) support the 1:2 sorption stoichiometry. These results indicate that electrical potential parameters derived from the Donnan model can be applied to predict metal binding onto bacterial surfaces over a wide range of pH and ionic strength conditions.

1. INTRODUCTION

In recent years, surface complexation modeling has been applied to predict trends of ion sorption at the bacteria–water interface (e.g., Fein et al., 1997; Fowle and Fein, 1999; Yee and Fein, 2001; Wightman et al., 2001; Daughney et al., 2001; Haas et al., 2001; Ngwenya et al., 2003). Formulation of these models depends on a description of the cell surface electrical double layer; therefore, one of the major requirements when using surface complexation models is the accurate representation of the bacterial surface electric field. Electrical charge on the cell surface arises from the ionization of proton-active functional groups attached to cell wall polymers. In gram-positive cell walls, ionizable functional groups are associated with peptidoglycan and secondary polymers such as teichoic or teichuronic acids. Carboxyl functional groups attached to the unlinked peptide crosslinks of peptidoglycan and phosphoryl groups associated with the teichoic acids can deprotonate to form negatively charged metal binding sites. These anionic functional groups generate charge in the cell wall which results in the formation of an electric field that surrounds the entire cell. The cell surface electric field controls the concentration and spatial distribution of ions and counterions at the cell–water interface, and can strongly affect metal binding onto the cell wall.

Small et al. (2001) have reported ionic strength dependent metal sorption onto bacterial surfaces, suggesting that interfacial electrostatic forces can affect microbial metal uptake. Previous efforts to quantify the effect of the cell surface electric field on metal–bacteria sorptive phenomena have been restricted to the Constant Capacitance and Stern models (Fein et al., 1997; Daughney and Fein, 1998). The Constant Capacitance model assumes that the surface potential is related linearly to the surface charge by the capacitance of the bacterial surface. This linear relationship is limited to high ionic strength conditions and generally cannot be extended to dilute electrolyte solutions. In contrast, the Stern model separates the surface electric field into two regions, a compact layer at the surface and a diffuse layer at some distance away from the interface. In the case of oxide mineral surfaces, the formation of outer-sphere complexes in the diffuse layer can account for ionic strength dependent metal sorption behavior (Davis and Kent, 1990; Dzombak and Morel, 1990). However, the Stern model was developed for ion-impenetrable planar surfaces, and does not accurately describe the electric field formed by three-dimensional permeable membranes such as bacterial cell walls (Poortinga et al., 2002). Therefore, the application of the Stern model to bacterial surfaces represents an empirical approach, and the resulting model parameters have limited physical meaning.

The surface potential generated by electrically charged microbial membranes can be accurately quantified using Donnan potential theory (Ohshima and Kondo, 1990; Wasserman and Felmy, 1998). The Donnan model assumes the cell wall is an ion-penetrable volume composed of homongeneous cross-linked ionizable functional groups. The deprotonation of these functional groups forms an electrical potential which extends across the membrane to the interface between the cell wall surface and bulk solution. Studies by Plette et al. (1995) and Martinez et al. (2002) have successfully applied this approach to correct for the electrostatic effects associated with proton

* Author to whom correspondence should be addressed (nyee@andromeda.rutgers.edu).

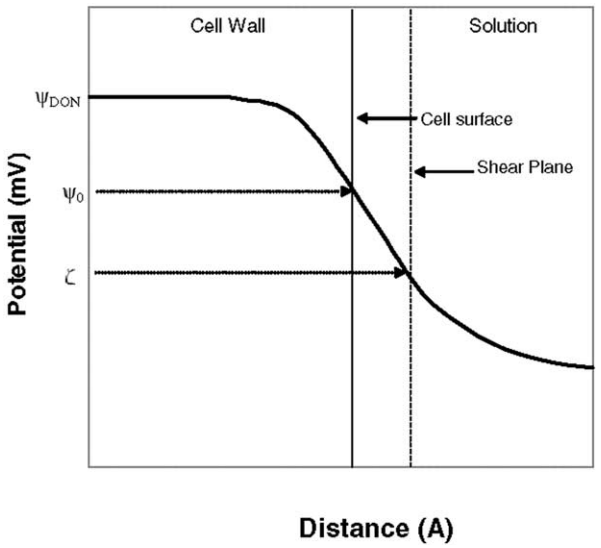

Fig. 1. Schematic representation of the potential profile across the cell wall of *B. subtilis*, where Ψ_{DON} is the Donnan potential, Ψ_0 is the surface potential, and ζ is the zeta potential.

binding onto bacterial cell walls. However, the extent to which Donnan potential theory can describe metal sorption data remains poorly understood.

In this study, we conducted electrophoretic mobility and acid–base titration experiments to characterize the surface electrical potential properties of the gram-positive bacteria species *Bacillus subtilis*. Metal sorption experiments with Ca(II), Sr(II), and Ba(II) in 0.1 mol/L to 0.001 mol/L KNO_3 solutions were also performed to examine the electrostatic interactions between metal ions and the cell surface electric field. The objective of this study was to determine surface potential parameters for *B. subtilis* and to test if Donnan potential theory can provide a means to describe surface potential dependent metal sorption effects.

2. THEORY

The electrical potential profile across the cell wall can be described using the Poisson-Boltzmann equations for the membrane and the solution (Ohshima and Kondo, 1990; Wasserman and Felmy, 1998) and is illustrated in Figure 1. The Donnan potential (Ψ_{DON}) is defined as the electrical potential within the cell wall, the surface potential (Ψ_0) is the electrical potential at the cell–water interface, and the zeta potential (ξ) is the electrical potential at the shear plane. The magnitude of the Donnan potential is controlled by the fixed charge excess within the cell wall. The charge excess, $[L^-]_T$ (μmol/mg), can be determined from acid–base titration experiments and is equal to the difference between the total added base and the equilibrium H^+ and OH^- ion concentrations at any given point on a titration curve:

$$[L^-]_T = C_a - C_b + [OH^-] - [H^+] \quad (1)$$

where C_a and C_b refer to the concentration of acid and base added, respectively. Here, we assume that the charge excess corresponds to the formation of deprotonated anionic functional groups in the cell wall. L_T therefore represents the total concentration of negatively charged cell wall metal binding sites. The type of cell wall functional group is not distinguished. The value of L_T changes as a function of pH and can be determined directly from the titration data. The corresponding cell wall charge ρ (C/m^3) is given by the following equation:

$$\rho = \frac{[L^-]_T F}{\eta \nu} \quad (2)$$

where F is Faraday's constant, η is the density of cells (cells/g), and ν is the cell wall volume (m^3/cell). We estimate a cell density of 6.7×10^{12} cells per gram dry mass of bacteria (Gonçalves et al., 1987) and a cell wall volume of 1.12 μm^3 per cell, based on a cell wall thickness of 25 nm (Beveridge, 1981) and a cylindrical cell geometry with a cell dimension of 1×5 μm. It should be noted that the calculation of the cell wall charge is highly sensitive to estimates of cell dimensions and cell density, and the resulting uncertainties can affect the surface potential calculation.

The complexation of metal ions with cell wall functional groups can be described with the following reaction:

$$xL^- + yMe^{2+} \Leftrightarrow L_x - Me_y^{(2y-x)} \quad (3)$$

where L^- is a deprotonated surface ligand, Me^{2+} is divalent metal cation, L_x-$Me_y^{(2y-x)}$ is a metal–ligand surface complex, and x and y are the stoichiometric coefficients for the surface ligand and metal, respectively. The distribution of metal between the solid and aqueous phase can be quantified using the corresponding mass action equation:

$$K_{app} = \frac{[L_x - Me_y^{(2y-x)}]}{[L^-]^x a_{Me2+}{}^y} \quad (4)$$

where K_{app} is the apparent equilibrium constant and a_{Me2+} is the activity of the metal ion determined using the Davies equation. K_{app} for each data point on the sorption isotherm can be solved in conjunction with the following mass balance equations:

$$[L^-]_T = [L^-] + [L_x - Me_y^{(2y-x)}] \quad (5)$$

$$[Me]_T = [Me^{2+}]_{aq} + [L_x - Me_y^{(2y-x)}]_s \quad (6)$$

where $[Me]_T$ is the total amount of metal added and $[Me^{2+}]_{aq}$ is the concentration of metal in the aqueous phase at equilibrium.

To find the intrinsic metal binding constants for metal ions bound to cell wall ligands, the apparent sorption constants must be corrected for the electrostatic potential in the cell wall. In this study, the cell wall potential was determined from the cell wall charge using the Donnan equation. We assume that the transition between the cell wall and solution is very thin compared to the thickness of the cell wall, such that the Donnan potential is constant across the cell wall and is approximately equal to the surface potential. The Donnan potential can be calculated using the following equation (Wonders et al., 1997):

$$\psi_{\mathrm{DON}} = \frac{RT}{zF}\mathrm{arcsinh}\left(\frac{\rho}{2zFc}\right) \quad (7)$$

where ρ is the cell wall charge, z is the valency of the symmetrical electrolyte, R is the universal gas constant, T is the absolute temperature, and c is the concentration of all ions in units moles per volume. The Donnan potential can then be applied to determine the Boltzmann correction factor and the intrinsic metal sorption constant:

$$K^{\mathrm{int}} = K^{app}exp\left(-\frac{\Delta ZF\psi_{DON}}{RT}\right) \quad (8)$$

where ΔZ is the change in charge of surface species and K_{intr} is the intrinsic equilibrium constant referenced to zero surface charge.

3. MATERIAL AND METHODS

3.1. Growth of Culture

Bacillus subtilis cells were harvested from pure cultures grown from trypticase soy broth, at 30°C for 16 h. After incubation, the cells were centrifuged in 250 mL in acid-washed and autoclaved 250-mL polypropylene bottles at 10,400 *g* at 20°C for 10 min. The nutrient medium was discarded, and the cells were rinsed five times by centriguation (10,400 *g* 10 min) in either a 0.1 mol/L, 0.01 mol/L, or 0.001 mol/L KNO_3 electrolyte solution, depending on the electrolyte concentration used in the experiments. The cells were then suspended in the corresponding electrolyte background solution.

3.2. Electrophoretic Mobility Experiments

The electrophoretic mobilities of *B. subtilis* were measured in 0.1 mol/L, 0.01 mol/L, and 0.001 mol/L KNO_3 at 25°C utilizing a laser-Doppler velocimetric device (Zetasizer 3000, Malvern Instruments, Southborough, MA). The instrument was calibrated with a single zeta potential transfer standard (silica colloids) of -50 ± 5 mV. The mobility of *B. subtilis* cells was determined with cell suspensions diluted to a solid-solution concentration of 5 mg bacteria/L (dry wt.). Velocity measurements were made as a function of pH with an applied field strength of 2500 V/m. The pH of the suspension was adjusted via the addition of small aliquots of standardized HNO_3 or KOH of similar ionic strength. The pH of the cell suspension was measured using an Orion PerpHecT 3in1 pH probe to ensure no electrode salt dripped into the solution. The average uncertainty of each measurement was less than 5% relative standard deviation. Mobility measurements were also made of *B. subtilis* cells sorbed with Ca(II), Sr(II), or Ba(II) to investigate the surface charging effects as a function of metal loading. These experiments were performed with cells suspended in a solution with a known amount of aqueous metal and following the same procedure as above.

3.3. Cell Wall Charge Determination

The total negative charge on *B. subtilis* cell wall was determined with acid–base titration experiments. Titrations were conducted using an auto-titrator assembly with cells suspended in three different electrolyte concentrations (0.1, 0.01, and 0.001 mol/L KNO_3). The electrolyte used was purged of dissolved CO_2 by bubbling N_2 gas for 1 h, and the experiments were conducted in a N_2 atmosphere. The titrations were carried out using a commercially supplied volumetric standard of 1.0005 mol/L HNO_3 and a carbonate-free 0.1058 mol/L NaOH solution standardized against the acid. To determine the total negative cell wall charge, the pH of the bacterial suspension first adjusted to the isoelectric point of the cells. The cell suspension was then allowed to equilibrate for 30 min before titration with NaOH up to pH 10. At each titration step, a stability of 0.1 mV/s was attained before the next aliquot of titrant was added. The dry mass of the cell suspension was determined by filtration through a 0.2-μm filter.

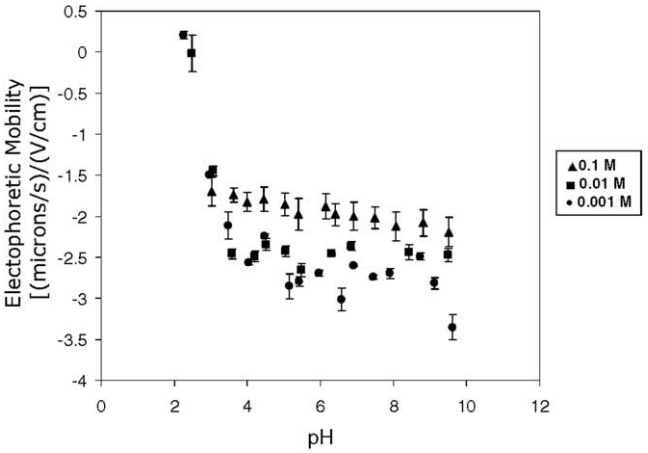

Fig. 2. Electrophoretic mobility of *B. subtilis* as a function of pH in 0.1 mol/L (▲), 0.01 mol/L (■), and 0.001 (●) mol/L KNO_3 electrolyte solutions.

3.4. Metal Binding Experiments

Ca(II), Sr(II), and Ba(II) binding experiments were performed as a function of pH in 0.1, 0.01, and 0.001 mol/L KNO_3 solutions. A cell suspension of a known cell concentration was placed in contact with 1.0 ppm of metal standard (Ca(II), Sr(II), or Ba(II)) in a sterilized 250-mL polypropylene bottle. The pH of suspension was adjusted to the desired value using 0.1 mol/L NaOH or HNO_3, and allowed to equilibrate 0.5 h. A 5-mL aliquot of the cell suspension was then sampled and filtered (0.45 μm). The concentration of Ca(II), Sr(II), and Ba(II) remaining in solution was determined by analyzing the filtrate using an inductively coupled plasma–atomic emission spectroscopy technique. The analytical uncertainty was determined to be approximately $\pm$ 5%. The amount of metal bound to cell was calculated as the difference between the initial metal concentration and metal concentration analyzed in the filtrate.

4. RESULTS AND DISCUSSION

4.1. Surface Potential Characterization

The electrophoretic mobility of *B. subtilis* measured in varying KNO_3 electrolyte solutions is shown in Figure 2. The data indicate that the cells are dominantly electronegative in the pH range studied. The magnitude of the electronegative mobility increases with increasing pH, and decreases with increasing electrolyte concentrations. The cells display a sharp increase in the magnitude of the electrophoretic mobility from pH 2.5 to 4, but level off at higher pH values. At neutral pH conditions, the absolute value of the mobility increases significantly from 0.1 mol/L to 0.01 mol/L KNO_3, but only slightly from 0.01 mol/L to 0.001 mol/L KNO_3.

The bacterial cells display an isoelectric point of approximately pH 2.4. At this pH condition, the concentration of negative charged surface sites is equal to the concentration of positively charged amino sites, and the net surface charge is equal to zero. As the pH increases from the isoelectric point, the acidic cell wall functional groups progressively deprotonate, generating a net negative charge within the cell wall and an electronegative potential on the cell surface.

The cell wall electrical potential is affected by the interactions between the electrolyte counter-ions and the cell surface electric field. At high electrolyte concentrations, electrostatic

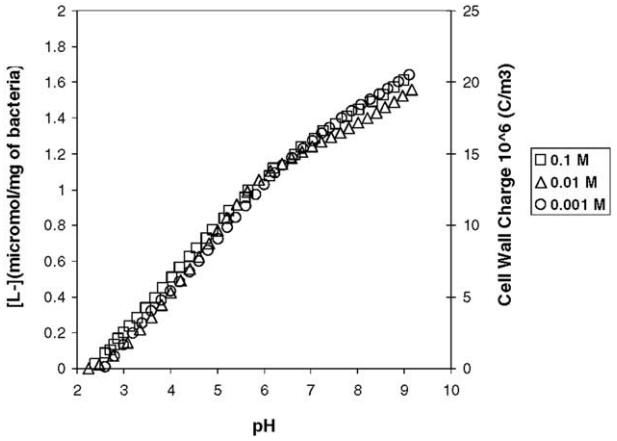

Fig. 3. Potentiometric titration curve for *B. subtilis* in 0.1 M to 0.001 M electrolyte solution.

sorption of K^+ counter-ions can satisfy the surface charge excess and decrease cell wall electrical potential. In contrast, dilute electrolyte concentrations allow the surface electric field to expand, which results in increasing electrophoretic velocities.

Electrophoretic mobility measurements can be used to calculate the zeta potential (ζ) for bacterial cells (van der Wal et al., 1997a) and serve as a proxy for the surface potential. However reliable estimates of ζ require an accurate knowledge of surface conductance effects (van der Wal et al., 1997b) which are currently unknown for *B. subtilis*. Ion conduction in the hydrodynamically stagnant layer can strongly affect electrokinetic behavior, and can explain why the electrophoretic mobility of *B. subtilis* is almost constant between pH 4 to 10 even though the cell wall charge changes considerably.

The acid–base titration data for *B. subtilis* are shown in Figure 3. The titration curves collected for *B. subtilis* in 0.1 mol/L to 0.001 mol/L KNO_3 solutions display nearly identical buffering capacities across the pH range studied. These results indicate that ionic strength has a weak effect on the acid–base behavior of the cell wall functional groups. The lack of ionic strength dependence on proton binding is likely due to the strong chemical bonds formed between the H^+ ions and the cell surface functional groups. Titration of the cells from pH 2.4 to 9 reveals a surface charge excess of 1.6 μmol/mg. At pH 2.4, the net surface charge is equal to zero, and the surface charge excess above this pH value can be used to determine the magnitude of negative charge per cell wall volume (C/m^3). The Donnan potential generated by the cell wall charge of *B. subtilis* was calculated using the Donnan equation and plotted on Figure 4. The calculations indicate that the cell wall potential increases with increasing pH, and decreases with increasing electrolyte concentrations. These trends are in qualitative agreement with the electrophoretic mobility measurements, and in close quantitative agreement with the Donnan potential values determined for the gram-positive bacteria *Bacillus brevis* by Wasserman and Felmy (1998).

4.2. Metal Sorption Experiments

Figure 5 is a plot of Ca(II), Sr(II), and Ba(II) sorption onto *B. subtilis* as a function of pH at three different electrolyte concentrations. The three alkaline earth metals display very similar metal sorption behavior. The extent of metal sorption increases with increasing pH, and decreases with increasing electrolyte concentration. The results show significant quantities of the metals sorbing onto the bacterial cell wall in 0.001 mol/L KNO_3 solutions, forming a distinct sorption edge between pH 4 to 6. At intermediate electrolyte concentrations

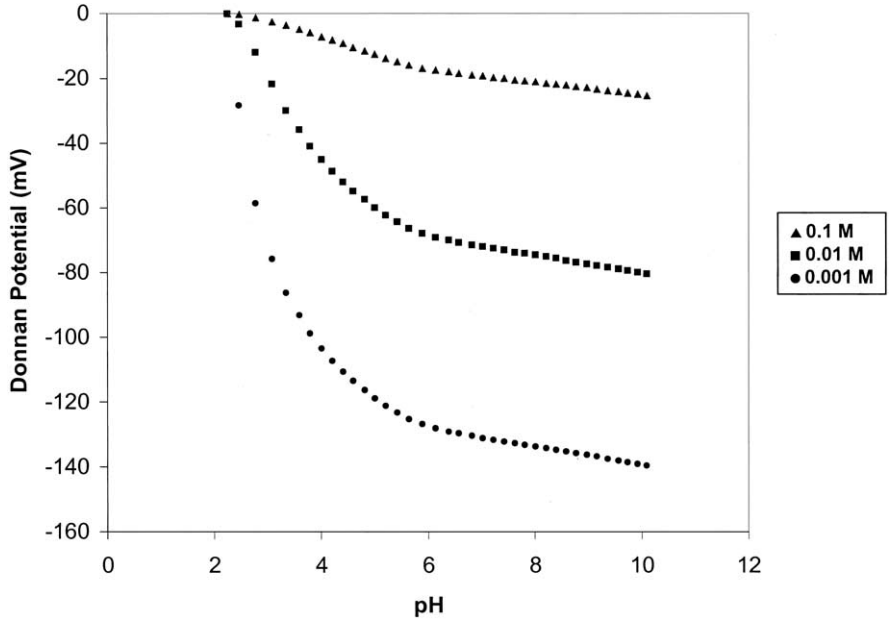

Fig. 4. Calculated Donnan potential as a function of pH in 0.1 mol/L (▲), 0.01 mol/L (■), and 0.001 (●) mol/L KNO_3 electrolyte solutions.

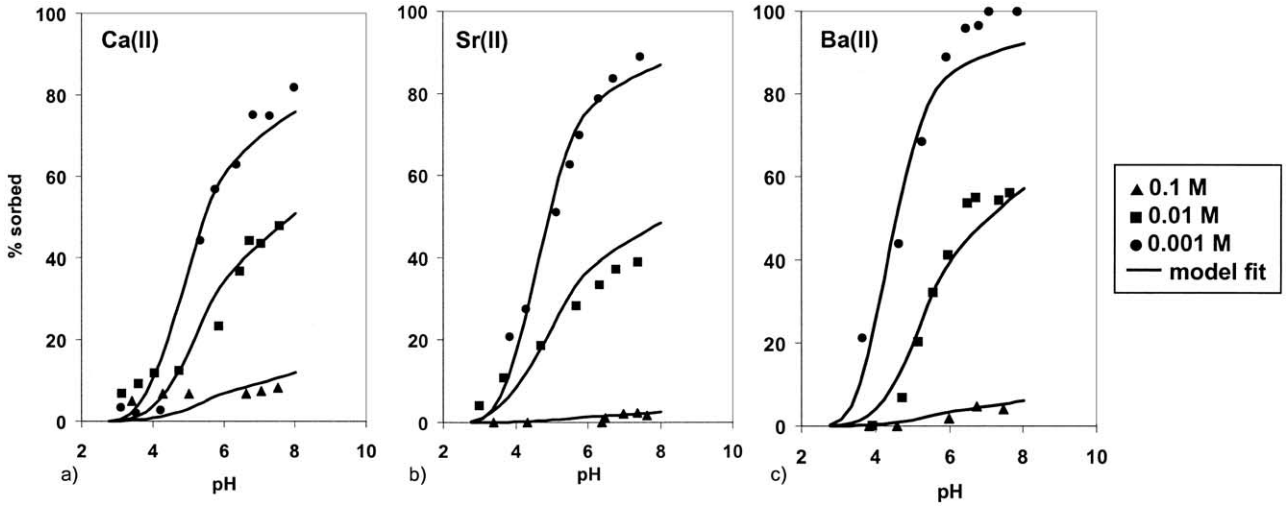

Fig. 5. Metal sorption onto 165 mg/L of *B. subtilis* as a function of pH in 0.1 mol/L (▲), 0.01 mol/L (■), and 0.001 mol/L (●) KNO_3 electrolyte solutions for (a) Ca(II), (b) Sr(II), and (c) Ba(II). The solid line represents the best-fit curve for each data set determined by the bidentate electrostatic model. See Table 1 for model parameters.

(0.01 mol/L), the overall amount of metal sorbed is reduced and the position of the sorption edge is shifted to higher pH values. At the highest ionic strength (0.1 mol/L), minimal sorption was measured (<10% $[Me]_{sorbed}$) and a sorption edge was not distinguishable.

The effect of pH on Ca(II), Sr(II), and Ba(II) sorption is similar to other metals studied for *B. subtilis* (Fein et al., 1997). At the metal:bacteria ratio used in these experiments, the position of the sorption edge is controlled by the pK_a value for proton dissociation of cell wall carboxyl functional groups (pK_a = 4.5). Below this pK_a value, the surface carboxyl groups are dominantly protonated. All three alkaline earth metals display a weak affinity for the cell wall at low pH, suggesting that metals do not form complexes with protonated cell wall functional groups. As pH increases, the carboxyl groups progressively deprotonate, forming negative cell wall charge. The attractive forces between the anionic surface sites and cationic metal ions result in the formation of metal–ligand cell wall complexes. At pH values above the carboxyl pK_a value, the cell wall carboxyl groups are dominantly deprotonated and extensive metal sorption is observed.

The ionic strength dependence of Ca(II), Sr(II), and Ba(II) sorption onto *B. subtilis* is characteristic of outer-sphere complexation. This sorption mechanism involves the formation of electrostatic bonds, where the metal ion retains its primary hydration shell upon sorption. Group 2A elements are hard acids and generally do not form covalent bonds. The adsorption of alkaline earth metals onto mineral surfaces has been shown to be strongly influenced by solution ionic strength, indicative of electrostatic bonding (Hayes and Leckie, 1987; Davis and Kent, 1990). On mineral surfaces, high ionic strength conditions cause the diffuse layer to collapse, thereby inhibiting the formation of outer-sphere complexes. Similarly, the sorption of alkaline earth metals onto bacterial surfaces is highly sensitive to the electrostatic effects. However, unlike mineral surfaces, the surface sites in the bacterial cell wall are distributed three-dimensionally and the electrical potential spans across the membrane. Therefore, on bacterial surfaces, hydrated metal cations can form outer-sphere complexes with anionic sites inside the bacterial cell wall. Additional spectroscopic work is required to determine the exact structure and local coordination of these surface complexes.

4.3. Surface Complexation Modeling

Both electrostatic and nonelectrostatic models with various stoichiometries were used to fit the experimental data. The average metal binding constants and standard deviations (1*s*) for each model are reported in Table 1. It is noted that the points outside the sorption edge (<10% $[Me]_{sorbed}$ and >90% $[Me]_{sorbed}$) provide the weakest constraint on the metal sorption constant. In general, the high ionic strength data (0.1 mol/L) yield the highest 1*s* errors due to the low amounts of metal sorbed and the large effect of analytical uncertainties on log *K* values.

The metal sorption data were first modeled with a nonelectrostatic model and 1:1 metal–ligand stoichiometry:

$$L^- + Me^{2+} \Leftrightarrow L - M^+ \quad (9)$$

Equation 4 was used to determine equilibrium constants for each metal and ionic strength condition. The log *K* values and 1*s* errors indicate that the nonelectrostatic model can adequately quantify the pH-dependent sorption effect. However, the apparent metal binding constants vary significantly with ionic strength. In the case of Sr(II), the log K_1^{app} values increases by over two orders of magnitude from 0.1 mol/L and 0.001 mol/L KNO_3 solutions. This increasing affinity of the metal to sorb onto the surface corresponds to the increase of cell wall potential with decreasing electrolyte concentrations. Because the nonelectrostatic model does not account for electrical potential effects, the log K_1^{app} values are ionic strength specific and limited to the electrolyte concentrations tested in the laboratory.

Intrinsic sorption constants were determined by correcting the apparent sorption constant with the Boltzmann factor. The

Table 1. Log K values for Ca(II), Sr(II), and Ba(II) sorption onto *B. subtilis*.

Metal	Electrolyte concentration	[a]log K_1^{app}	log K_1^{int}	log K_2^{app}	log K_2^{int}
Ca(II)	0.1 M	2.5 ± 0.4[b]	2.2 ± 0.5	6.2 ± 0.7	5.9 ± 0.8
	0.01 M	3.4 ± 0.2	2.3 ± 0.2	7.2 ± 0.2	6.1 ± 0.2
	0.001 M	4.1 ± 0.2	1.9 ± 0.2	7.8 ± 0.2	5.7 ± 0.1
	average[c]		2.1 ± 0.3		5.9 ± 0.3
Sr(II)	0.1 M	1.7 ± 0.7	1.4 ± 0.7	5.4 ± 0.7	5.0 ± 0.7
	0.01 M	3.4 ± 0.1	2.4 ± 0.1	7.3 ± 0.1	6.3 ± 0.2
	0.001 M	4.1 ± 0.3	2.0 ± 0.2	8.0 ± 0.2	5.9 ± 0.2
	average		2.1 ± 0.2		6.0 ± 0.2
Ba(II)	0.1 M	2.2 ± 0.9	1.9 ± 0.9	6.1 ± 0.9	5.7 ± 0.9
	0.01 M	3.6 ± 0.2	2.4 ± 0.2	7.4 ± 0.2	6.2 ± 0.1
	0.001 M	4.1 ± 0.4	2.2 ± 0.2	8.1 ± 0.3	6.2 ± 0.2
	average		2.3 ± 0.2		6.2 ± 0.2

[a] Superscript indicates apparent or intrinsic log K value; subscript indicates 1:1 or 1:2 sorption stoichiometry.
[b] Average log K value with 1*s* error at each electrolyte concentration.
[c] Overall average log K^{int} for all electrolyte concentrations, calculated with the data on the sorption edge only (e.g., between 10–90% $[Me]_{sorbed}$).

log K_1^{int} values for Ca(II), Sr(II), and Ba(II) are 2.1 ± 0.3, 2.1 ± 0.2, and 2.3 ± 0.2, respectively. The modeling results show that the intrinsic sorption constants are invariant to ionic strength, indicating that the Boltzmann factor and Ψ_{DON} can successfully describe surface potential effects. This result suggests that only one constant is required to describe the pH and ionic strength effect on metal sorption. Previous studies have determined intrinsic sorption constants for Ca(II) and Sr(II) onto *B. subtilis* in high ionic strength solutions (0.1 mol/L $NaClO_4$ electrolyte) using the Constant Capacitance model and a capacitance value of 8 F/m^2 (Fowle and Fein, 1999; Fein et al., 2001). Fowle and Fein (1999) reported a log K^{int} value of 2.8 for Ca(II), and Fein et al. (2001) reported a log K^{int} value of 2.6 for Sr(II). These values are slightly higher than those determined using the Donnan model, suggesting that the Constant Capacitance model provides a lower estimate of the cell surface electrical potential. The discrepancy in values may be partly explained by the fact that the Constant Capacitance model describes the electrical double layer properties of ion impenetrable surfaces (e.g., mineral surfaces) and provides a poor physical representation of the bacterial cell wall. For example, the value of 8 F/m^2 for the cell surface capacitance is an empirically derived fit parameter (Fein et al., 1997), and is unrealistically high compared to capacitance values determined by direct electrophysical measurements of biologic membranes (Pethig, 1979; Holzël, 1999).

A 1:2 metal–ligand ratio was also used to fit the data, according to the following stoichiometry:

$$2L^- + Me^{2+} \Leftrightarrow L_2 - M^0 \qquad (10)$$

The model yields log K_2^{int}values for Ca(II), Sr(II), and Ba(II) of 5.9 ± 0.3, 6.0 ± 0.2, and 6.2 ± 0.2, respectively. The model fits are displayed in Figure 5. Compared to the 1:1 stiochiometry, 1:2 metal–ligand model fit reduces the relative 1*s* error of the sorption constants. Analysis of the 1*s* values of all the models tested indicates that the 1:2 stoichiometry provides the best fit to the experimental data.

To determine the validity of the 1:2 metal–ligand stoichiometry, electrophoretic mobility experiments were conducted with *B. subtilis* cells sorbed with Ca(II), Sr(II), and Ba(II) (Fig. 6). According to the 1:2 reaction stoichiometry, the metal ions are

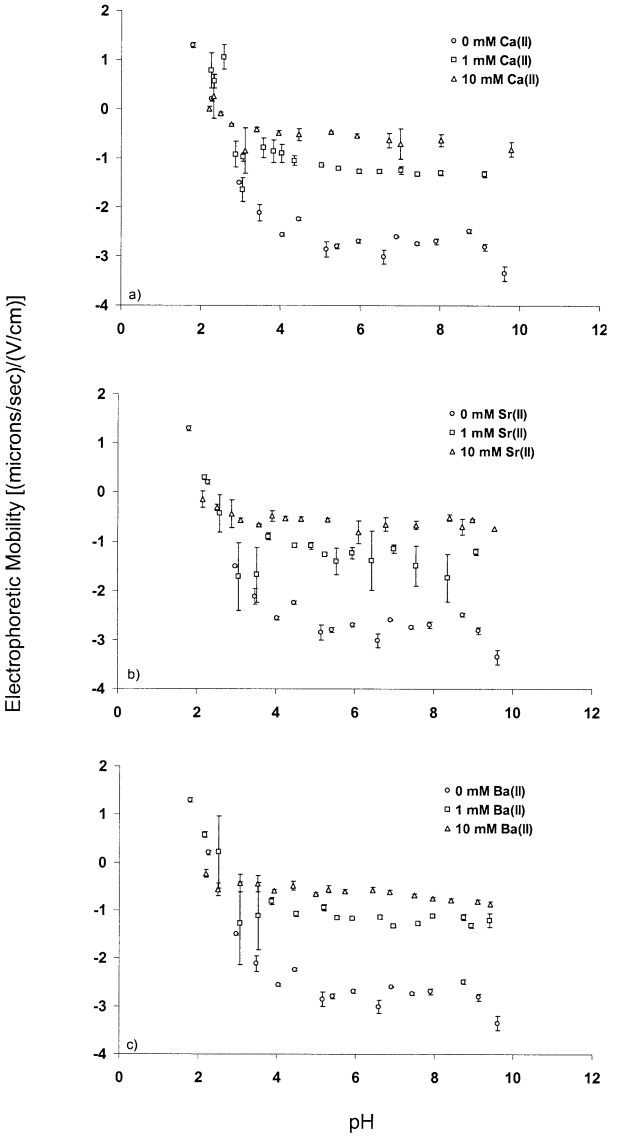

Fig. 6. Electrophoretic mobility of 5 mg/L of *B. subtilis* cells suspended in 0 mM (●), 1 mM (■) and 10 mM (▲) metal solutions of (a) Ca(II), (b) Sr(II), and (c) Ba(II).

electrostatically sorbed to the cell wall to satisfy charge excess at the cell–water interface. This reaction involves the electrostatic bonding of one divalent metal to two deprotonated surface functional groups, resulting in the formation of a surface complex with neutral charge (Eqn. 10). Therefore, increasing metal sorption decreases the magnitude of electronegative surface potential, and at site saturation the surface potential is neutral. Conversely, a 1:1 sorption stoichiometry involves the bonding of one divalent metal with one deprotonated surface functional group, resulting in the formation of a positively charged metal:ligand surface complex (Eqn. 9). This stoichiometry leads to charge reversal at high surface coverage, and can occur only if there are specific chemical interactions between the metal ions and cell wall functional groups.

The electrophoretic mobility measurements of *B. subtilis* cells sorbed with high concentrations of alkaline earth metals indicate that charge reversal does not occur (Fig. 6). In the absence of metal ions, the cells display strong electronegative mobility, with the magnitude of the mobility increasing with increasing pH. In the presence of Ca(II), Sr(II), or Ba(II), the magnitude of the mobility decreases with increasing metal concentrations and approaches zero at the highest metal concentration. At 10 mM, the concentration of metal in solution is approximately 10^3 times higher than the concentration of surface sites in the bacterial cell wall, and the surface sites are nearly saturated with divalent cations. Under these conditions, minimal electrophoretic mobility was measured across the pH range studied, indicating that at high surface coverage, the surface potential approaches electrical neutrality. Contrary to previous surface charge calculations for Ca(II) binding onto gram-positive cell walls by Plette et al. (1996), no charge reversal was observed. The electrophoretic mobility trends reported here are in agreement with earlier zeta potential measurements for *B. subtilis* conducted with Ca(II), Sr(II), and Ba(II) solutions by Chang and Hsieh (1991). The lack of charge reversal at high metal loading is consistent with a 1:2 metal–ligand sorption stoichiometry and an electrostatic bonding mechanism.

The metal binding constants for Ca(II), Sr(II), and Ba(II) can be separated into their intrinsic and electrostatic components. The Gibbs Free Energy of the sorption reaction can be represented as the sum of chemical and electrostatic components such that:

$$\Delta G_{sorption} = \Delta G_{chemical} + \Delta G_{electrostatic} \quad (11)$$

where $\Delta G_{sorption}$ is related to apparent sorption constant; the $\Delta G_{chemical}$ term is related to the specific interactions between the metal ions and cell wall ligands, and determines the intrinsic metal bind constant; and the $\Delta G_{electrostatic}$ term describes the effect of the bacterial surface electric field on metal uptake. The intrinsic chemical component does not vary at different electrolyte concentrations, and remains constant as a function of ionic strength. Under high ionic strength conditions, the electrostatic driving force is low and the chemical component dominant. However, at these electrolyte concentrations minimal sorption was observed, suggesting that Ca(II), Sr(II), and Ba(II) do not form strong chemical bonds with specific cell wall ligands. Conversely, in dilute electrolyte solutions, the electrostatic driving force is high and extensive sorption was measured, indicating that it is the change in the electrostatic component which drives the sorption reaction.

5. CONCLUSIONS

The results of this study demonstrate that electrostatic effects can play an important role in sorption processes at the cell–water interface. Sorption experiments conducted with alkaline earth metals exhibit a strong dependence on cell wall electrical potential, suggesting that the metal ions are bound to the bacterial cell wall via an outer-sphere complexation mechanism. Quantification of the electrical potential effects on metal sorption using the Donnan model yields excellent fits to the experimental data and allows for the determination of intrinsic metal binding constants. Because of its simple and numerically efficient formulation, the Donnan equation can be readily incorporated into existing geochemical speciation codes. Application of geochemical speciation models to microbial surfaces also requires reliable estimates for surface sites pK_a values and relative functional group concentrations. The integration of these surface complexation parameters with the Donnan model will allow for prediction of ion sorption onto microorganisms over a wide range of pH and ionic strength conditions.

Acknowledgments—This research was funded by The Leverhulme Trust grant number F-00122/F (N.Y.), the Canada Research Chairs Program and NSERC (D.F.). We gratefully acknowledge the work of Tom J. Collins for acquiring the mobility data and Ezra Kulczycki for his help with the acid–base titration experiments. We also thank three anonymous reviewers for their insightful comments.

Associate editor: J. Haas

REFERENCES

Beveridge T. J. (1981) Ultrastructure, chemistry, and function of the bacterial wall. *Int. Rev. Cytol.* **72,** 229–317.

Chang Y. I. and Hsieh C. Y. (1991) The effect of cationic electrolytes on the electrophoretic properties of bacterial cells. *Colloid Surf.* **53**.

Daughney C. D. and Fein J. B. (1998) The effects of ionic strength on the adsorption of H^+, Cd^{2+}, Pb^{2+} and Cu^{2+} by *Bacillus subtilis* and *Bacillus licheniformis*: A surface complexation model. *J. Colloid Interf. Sci.* **198,** 53–77.

Daughney C. J., Fowle D. A., and Fortin D. E. (2001) The effect of growth phase on proton and metal adsorption by *Bacillus subtilis*. *Geochim. Cosmochim. Acta* **65,** 1025–1035.

Davis J. A. and Kent D. B. (1990) Surface complexation modeling in aqueous geochemistry. In *Mineral–Water Interface Geochemistry* (eds. M. F. Hochella, Jr. and A. F. White). *Rev. Mineral* **23,** 177–260. Min. Soc. Am.

Dzombak D. A. and Morel F. M. M. (1990) *Surface Complexation Modeling: Hydrous Ferris Oxide*. John Wiley, New York.

Fein J. B., Daughney C. J., Yee N., and Davis T. (1997) A chemical equilibrium model for metal adsorption onto bacteria surfaces. *Geochim. Cosmochim. Acta* **61,** 3319–3328.

Fein J. B., Martin A. M., and Wightman P. G. (2001) Metal adsorption onto bacterial surfaces: Development of a predictive approach. *Geochim. Cosmochim. Acta* **65,** 4267–4273.

Fowle D. A. and Fein J. B. (1999) Competitive adsorption of metal cations onto two gram positive bacteria: Testing the chemical equilibrium model. *Geochim. Cosmochim. Acta* **63,** 3059–3067.

Gonçalves M. L. S., Sigg L., Reulinger M., and Stumm W. (1987) Metal ion binding by biological surfaces: Voltammetric assessment in the presence of bacteria. *Sci. Tot. Environ.* **60,** 105–119.

Haas J. R., Dichristina T. J., and Wade R. (2001) Thermodynamics of U(VI) sorption onto *Shewanella putrefaciens*. *Chem. Geol.* **180,** 33–54.

Hayes K. F. and Leckie J. O. (1987) Modeling ionic strength effects on cation adsorption at hydrous oxide/solution interfaces. *J. Colloid Interf. Sci.* **115,** 564–572.

Holzël R. (1999) Non-invasive determination of bacterial single cell properties by electrorotation. *Biochim. Biophys. Acta* **250,** 53–60.

Martinez R. E., Smith D. S., Kulczycki E., and Ferris F. G. (2002) Determination of intrinsic bacterial surface acidity constants using a donnan shell model and a continuous pKa distribution method. *J. Colloid Interf. Sci.* **253,** 130–139.

Ngwenya B. T., Sutherland I. W., and Kennedy L. (2003) Comparison of the acid-base behaviour and metal adsorption characteristics of a gram-negative bacterium with other strains. *Appl. Geochem.* **18,** 527–538.

Ohshima H. and Kondo T. (1990) Relationship among the surface potential, Donnan potential, surface free energy and charge density of ion-penetrable membranes. *Biophys. Chem.* **38,** 117–122.

Pethig R. (1979) *Dielectric and Electronic Properties of Biological Material*. John Wiley and Sons, Chichester.

Plette A. C. C., Benedetti M. F., Van Riemsdijk W. H., and Van der Wal A. (1995) pH dependent charging behavior of isolated cell walls of a gram-positive soil bacterium. *J. Colloid Interf. Sci.* **171,** 354–363.

Plette A. C. C., Benedetti M. F., and Van Reimsdijk W. H. (1996) Competitive binding of protons, calcium, cadmium, and zinc to isolated cell walls of a gram-positive soil bacterium. *Environ. Sci. Technol.* **30,** 1902–1910.

Poortinga A. T., Bos R., Norde W., and Busscher H. J. (2002) Electrical double layer interactions in bacterial adhesion to surfaces. *Surf. Sci. Reports* **47,** 1–32.

Small T. D., Warren L. A., and Ferris F. G. (2001) Influence of ionic strength on strontium sorption to bacteria, Fe(III) oxide, and composite bacteria-Fe(III) oxide surfaces. *Appl. Geochem.* **16,** 939–946.

van der Wal A., Minor M., Norde W., Zehnder A. J. B., and Lyklema J. (1997a) Electrokinetic potential of bacterial cells. *Langmuir* **13,** 165–171.

van der Wal A., Minor M., Norde W., Zehnder A. J. B., and Lyklema J. (1997b) Conductivity and dielectric dispersion of gram-positive bacterial cells. *J. Colloid Interf. Sci.* **186,** 71–79.

Wasserman E. and Felmy A. R. (1998) Computation of the electrical double layer properties of semipermeable membranes in multicomponent electrolytes. *Appl. Environ. Microbiol.* **64,** 2295–2300.

Wightman P. G., Fein J. B., Wesolowski D. J., Phelps T. J., Benezeth P., and Palmer D. A. (2001) Measurement of bacterial surface protonation constants for two species at elevated temperatures. *Geochim. Cosmochim. Acta* **65,** 3657–3669.

Wonders J. H. A. M., VanLeeuwen H. P., and Lyklema J. (1997) Metal- and proton-binding properties of a core-shell latex: Interpretation in terms of colloid surface models. *Colloids Surf. A* **120,** 221–233.

Yee N. and Fein J. (2001) Cd adsorption onto bacterial surfaces: A universal adsorption edge? *Geochim. Cosmochim. Acta* **65,** 2037–2042.